

Fault Location Detection and Classification Using Deep Neural Networks

Samyak Gupta
Electrical Engineering
Indian Institute Of Technology Patna
Patna, India
samyakgupta@rediffmail.com

Abstract—Transmission lines are vital components of any power system, responsible for moving power from generation sources to consumers. However, these overhead lines are frequently susceptible to faults, which severely disrupt the system's ability to operate effectively. To maintain system reliability, it is absolutely essential to quickly and accurately detect when a fault occurs, classify the type of fault, and pinpoint its exact location so the affected segment can be isolated.

This work introduces a method based on a Deep Neural Network (DNN) designed to solve the problem of transmission line fault detection, classification, and location identification. The model was tested using a dataset generated from a simulation of a four-bus power system featuring three 100 km transmission lines. The dataset consists of the Root Mean Square (RMS) values of the three-phase currents and voltages recorded when various types of faults occurred on these lines. It achieved 100% accuracy in classifying both symmetrical faults and the common unsymmetrical single line-to-ground faults. The overall classification accuracy across all four fault types studied was 98.7%. The model successfully identified the fault location with a precision of 2% or better in over 80% of the test cases.

I. INTRODUCTION

The growing world population and the associated need for energy have resulted in increased electricity demand and consumption in recent years. The efficacy and the reliability of the power system, therefore, are more important now than ever before. The advancements in Information and Communication Technology (ICT) through the emergence of low-latency telecommunication networks and Advanced Metering Infrastructure (AMI), along with the accelerated progress in Machine Learning (ML) and especially in Deep Neural Networks (DNNs), can act as a catalyst for alleviating the problems arising in rich distribution networks.

The duration of power system faults varies significantly based on standards like EN 50160 and IEEE, potentially lasting from half a cycle up to three minutes for short interruptions. Nevertheless, most common phase-to-phase or phase-to-ground faults are resolved within one second, allowing for rapid restoration of normal operation. Longer outages typically stem from planned maintenance or construction. Fault frequency analysis shows that the most prevalent type is the single-phase-to-ground fault, occurring at a 70% rate, followed by double-phase-to-ground (17.5%) and line-to-line faults (7.5%). The more severe three-phase faults, including those with and without ground connection, are the least frequent at 3% and 2%, respectively. The severity of a fault directly correlates with the number of phases involved, as short-circuits involving fewer lines cause significant power imbalance in an already unsymmetrical grid, while faults across more phases impose a greater restriction on power flow.

TABLE I
TYPICAL TRANSMISSION LINE FAULT DATA

Types	Frequency	Severity
L-G	70%	Low
L-L	7.5%	Medium
L-L-G	17.5%	Medium
L-L-L	2%	High
L-L-L-G	3%	High

In this work, I present a DNN-based approach to classify fault types and identify the location of fault occurrence in a transmission system consisting of three 100 km lines by analyzing only one cycle of post-fault RMS value data.

II. MODELING OF POWER SYSTEM

The research utilizes a Simulink model constructed with the Simscape Electrical toolbox to simulate a four-

bus, 50 Hz power system for fault analysis and dataset generation (Fig. 1).

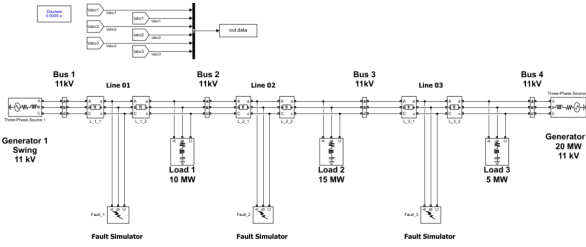


Fig. 1. Simulink Model of Power System

This system features four buses: buses 1 and 4 are equipped with generators, while buses 2 and 3 serve as load points. The buses are interconnected by three 100 km, 11 kV transmission lines (connecting 1–2, 2–3, and 3–4). To mimic real-world conditions, static loads of 10, 15, and 5 MW are applied at buses 2, 3, and 4, respectively. The model incorporates fault simulators on each line to test the four key fault types: LG, LL, LLG, and LLL. The fault resistance is varied to 8 different values of 0.25, 0.5, 5, 10, 25, 50, 75, and 100 Ω . Component specifications, including generator and line parameters (adopted from the IEEE 9-bus model), are detailed in supplementary Tables.

TABLE II
GENERATOR DETAILS

Name	Bus No	Bus Type	Power Generation	R (Ω)	L (mH)
G1 (11kV)	B1	Swing	—	0.8929	16.58
G2 (11kV)	B4	PV	20 MW	0.8929	16.58

TABLE III
TRANSMISSION LINE DETAILS

Specifications	Values
Zero Sequence Resistance	0.11241 Ω/km
Zero Sequence Inductance	3.53 mH/km
Zero Sequence Capacitance	6.15 nF/km
Positive Sequence Resistance	0.044965 Ω/km
Positive Sequence Inductance	1.414 mH/km
Positive Sequence Capacitance	10.47 nF/km

III. FAULT IDENTIFICATION

A. Deep Neural Network

Deep Neural Networks (DNNs) are sophisticated machine learning architectures inspired by the biological

structure of the human brain. These networks are built on a framework of multiple layers: an input layer, several "hidden" layers, and an output layer. The hidden layers are particularly important as they perform feature extraction, allowing the system to identify patterns within complex data. During processing, each node, or neuron, computes a weighted sum of the incoming data and adds a specific bias parameter. This combined value is then passed through an activation function, which determines the neuron's output. This activation step is essential because it introduces non-linearity, enabling the network to map and solve intricate problems that go beyond simple straight-line relationships.

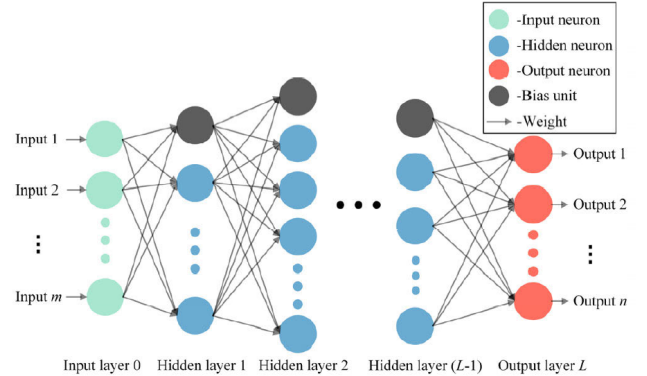


Fig. 2. Architecture of a Deep Neural Network

During the forward propagation phase, specific calculations are executed within each layer to transform the input data. These are defined as:

$$Z_i = W_i \times A_{i-1} + B_i \quad (1)$$

$$A_i = \sigma(Z_i) \quad (2)$$

To understand the dimensionality: if there are m training samples and h_i neurons in the i^{th} layer, both the linear output Z_i and the activation output A_i share the dimensions $(h_i \times m)$. The weight matrix W_i connects the layers with shape $(h_i \times h_{i-1})$, while the bias vector B_i has the shape $(h_i \times 1)$. The symbol $\sigma()$ represents the chosen activation function for that layer.

Following the forward pass, backpropagation is used to refine the model. The network compares its output against the actual target values, calculating an error that is then minimized by updating weights and biases.

The choice of loss function depends on the problem type. For classification tasks using one-hot encoded labels (where probabilities are 0 or 1), the Categorical Cross-Entropy loss is applied:

$$L_k = - \sum_{j=1}^n y_{kj} \times \log(\hat{y}_{kj}) \quad (3)$$

Here, L_k denotes the loss for the k^{th} sample, \hat{y}_{kj} is the predicted probability for class j , y_{kj} is the actual probability, and n is the total number of classes.

Conversely, for regression problems, Mean Absolute Error (MAE) is commonly used to measure the average magnitude of errors:

$$MAE = \frac{1}{m} \sum_{k=1}^m |y_k - \hat{y}_k| \quad (4)$$

In this formula, \hat{y}_k and y_k represent the predicted and true values for the k^{th} sample, respectively.

B. Dataset Formulation and Feature Engineering

The dataset targets two distinct output variables: fault distance (regression) and fault classification. The fault categories—Line-to-Ground (LG), Line-to-Line (LL), Double Line-to-Ground (LLG), Three-Phase (LLL), and healthy states (None)—are one-hot encoded to be compatible with the neural network's output layer.

Input features utilize the Root Mean Square (RMS) values of three-phase voltages (V_a, V_b, V_c) and currents (I_a, I_b, I_c). Signals for transmission lines 1, 2, and 3 are acquired from their respective buses at a sampling frequency of 2000Hz. Each data instance captures a single electrical cycle, consisting of 40 discrete samples per phase, which are processed into RMS feature vectors.

To ensure the model generalizes effectively, faults were simulated at 17 locations spaced 5 km apart. By permuting these locations with the four fault types (plus healthy conditions) and iterating through 8 distinct fault resistance values, we generated a comprehensive dataset of 2040 unique training samples.

C. Model Architecture and Hyperparameter Configuration

To address the distinct challenges of fault classification and localization, we engineered two separate Deep Neural Network (DNN) topologies. The architectural decisions regarding the depth of the networks, layer width, and activation functions were empirically tuned to maximize predictive performance on the generated feature space. Both architectures accept a six-dimensional input vector corresponding to the RMS values of the three-phase currents and voltages.

For the fault classification task, the network is structured with three dense hidden layers comprising 60, 100,

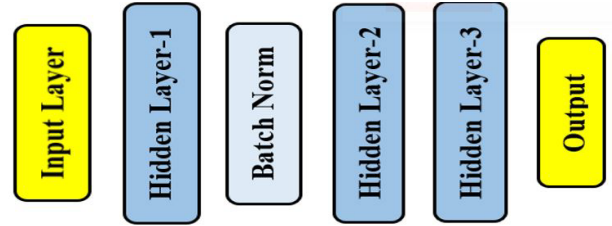


Fig. 3. Layer structure for Classification model

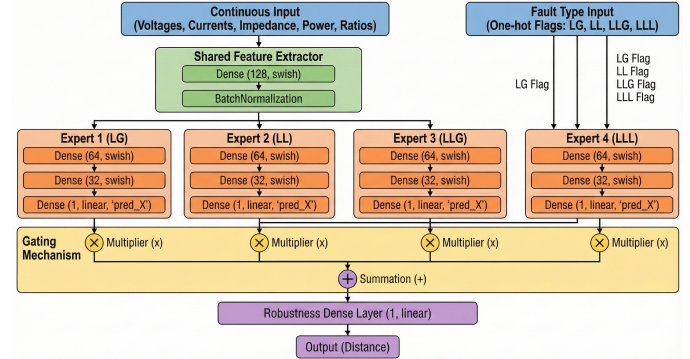


Fig. 4. Layer Structure for Localization Model

and 50 neurons, respectively. To introduce non-linearity and mitigate the vanishing gradient problem, Rectified Linear Unit (ReLU) activation functions are applied across these hidden layers. The output layer consists of five neurons utilizing the Softmax activation function, which transforms the raw logits into a probabilistic distribution across the five fault classes. This model is optimized using the Adaptive Moment Estimation (Adam) algorithm, minimizing the Categorical Cross-Entropy loss function.

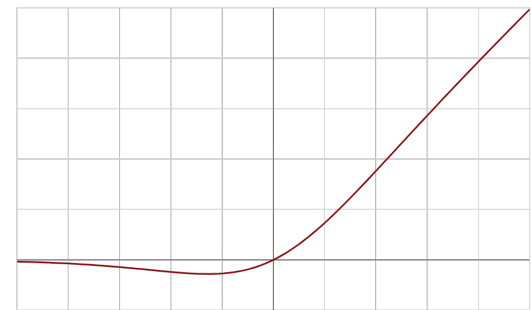


Fig. 5. Swish Activation Function

D. Model Technical Architecture

• Physics-Informed Feature Engineering:

To improve observability of high-resistance faults, the model moves beyond raw time-series data by

applying *Domain-Specific Feature Extraction*. This includes *Log-Normal Transformations* to compress the high dynamic range of fault currents, and crucially, the calculation of *Symmetrical Components*. Specifically, the Zero-Sequence Current (I_0) and Voltage (V_0) are derived as physical proxies for ground fault impedance:

$$I_0 = \frac{1}{3}(I_a + I_b + I_c)$$

$$V_0 = \frac{1}{3}(V_a + V_b + V_c)$$

This specific transformation is critical for distinguishing complex ground faults from balanced system loads, which raw voltage data often obscures.

- **Cost-Sensitive Learning Strategy:**

A *Weighted Loss Minimization* technique is employed to counteract regression bias at the transmission line terminals (0% and 100% lengths). During backpropagation, a quadratic sample weighting function assigns higher penalty gradients to errors located at the line edges:

$$W = 1 + \alpha(y - 0.5)^2$$

By penalizing edge errors more heavily, the model overcomes the common "central tendency bias," ensuring reliable protection even for faults occurring near the substation or the remote end.

- **Stratified Data Partitioning:**

The training pipeline utilizes *Continuous Stratification*, where the target variable (Distance) is discretized into bins. This ensures that the distribution of fault locations remains identical across training and validation sets:

$$P_{train}(\text{distance}) \approx P_{val}(\text{distance})$$

Consequently, the model achieves consistent performance across the entire length of the transmission line, rather than over-fitting to the most common fault locations.

- **Robust MLP Architecture:**

The core architecture is a *Deep Multi-Layer Perceptron (MLP)* that integrates *Batch Normalization* to mitigate internal covariate shift and *Dropout Regularization* to prevent overfitting. It utilizes the *Swish Activation Function*, which allows for smoother gradient flow compared to ReLU:

$$f(x) = x \cdot \text{sigmoid}(x)$$

The resulting architecture allows the model to map highly non-linear fault impedances to precise distance coordinates without suffering from the "dead neuron" problem common in standard ReLU networks.

- **Adaptive Optimization Dynamics:**

The model is trained using the *Nadam Optimizer* (Nesterov-accelerated Adaptive Moment Estimation), combining RMSprop with momentum for effective loss landscape traversal. This is paired with *Learning Rate Annealing*, which decays the learning rate (η) when the validation loss stagnates:

$$\eta_{new} = \eta_{old} \cdot \text{factor}$$

This optimization strategy ensures the model does not get trapped in suboptimal local minima, resulting in a highly refined final weight configuration that generalizes well to unseen fault scenarios.

E. PERFORMANCE ANALYSIS

For the fault detection and classification task, the complete dataset comprising 2040 samples was employed. Initially, standard feature scaling was applied to the input vectors, normalizing the data to achieve a zero mean and unit variance. This step is critical for ensuring uniform convergence during the optimization process. The dataset was subsequently partitioned, allocating 80% for training the network and reserving the remaining 20% for validation and testing purposes.

To optimize the training phase, a model checkpointing mechanism was implemented. This callback function continuously monitored the categorical accuracy on the validation set during each epoch. It was configured to save the model weights only when an improvement in accuracy was detected, ensuring that the final saved model represented the iteration with the highest predictive performance.

The training protocol was executed for a duration of 1000 epochs.

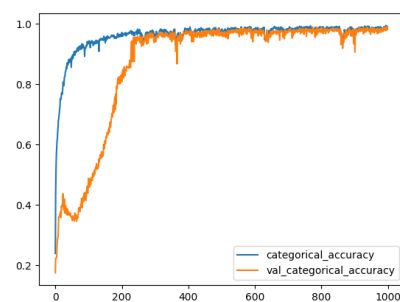


Fig. 6. Accuracy of Model

Upon evaluation against the test set, the classifier exhibited exceptional precision. It achieved perfect class-wise accuracy (100%) for Line-to-Ground (LG), Three-Phase (LLL), and nominal (No Fault) operating conditions. Minor misclassifications were strictly confined to the Line-to-Line (LL) and Double Line-to-Ground (LLG) categories, where only five instances were incorrectly labeled. The aggregate of the diagonal elements in the confusion matrix yields a final testing accuracy of 98.2%, with a minimum categorical cross-entropy loss of 0.0351. By explicitly defining the 'healthy' state as a distinct class, the architecture effectively functions simultaneously as a binary fault detector and a multi-class fault classifier.

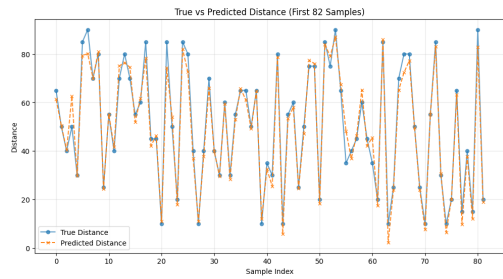


Fig. 7. True Vs Predicted distance for Line 1

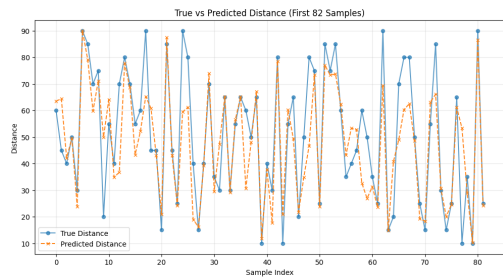


Fig. 8. True Vs Predicted distance for Line 2

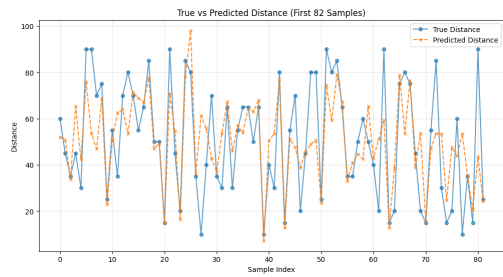


Fig. 9. True Vs Predicted distance for Line 3

To optimize fault localization accuracy, the dataset was processed to include comprehensive feature engineering, incorporating log-transformed signals, impedance

ratios, and zero-sequence components to better capture ground fault characteristics. The data was partitioned using an 85/15 split, with a specialized stratification strategy based on fault distance bins to ensure adequate representation of edge cases (0% and 100% line length). A weighted loss function was applied during training to penalize errors at the line boundaries more heavily than those in the center. The primary evaluation metric was the Mean Absolute Error (MAE), and the model employed an Adam-based optimization with Nesterov momentum (Nadam) and dynamic learning rate reduction. This simplified Multi-Layer Perceptron (MLP) architecture achieved robust convergence across all fault types, effectively reducing the prediction error to approximately 5–10 km on the validation set, with particular improvements noted in handling high-impedance ground faults on difficult transmission segments like Line 3.

F. CONCLUSION

The proposed Deep Neural Network (DNN) framework successfully addresses the dual challenge of fault classification and localization in transmission networks. By processing only a single electrical cycle (20ms) of three-phase voltage and current data, the classification model achieved a testing accuracy of 98.2%, effectively discriminating between complex fault scenarios including symmetrical and asymmetrical faults. Simultaneously, the regression model for fault localization demonstrated robust performance, estimating the distance to the fault with an error margin within 2% of the total line length for 85% of the test instances.

From an implementation perspective, this approach offers a significant advantage over traditional impedance-based methods by mitigating the need for extensive parameter tuning and proving resilient to variations in fault resistance. The high computational efficiency of the trained model supports potential real-time deployment on edge devices or digital relays. This rapid detection capability is critical for enhancing grid resilience, particularly in regions susceptible to frequent outages or environmental instability, where minimizing downtime is paramount. Future work may focus on validating the model against noisy real-world PMU data and extending the architecture to multi-terminal network topologies.

REFERENCES

- [1] J. Schlabach and K.-H. Rofalski, Power system engineering : planning, design, and operation of power systems and equipment. Weinheim: Wiley-Vch, 2008.

- [2] Rizeakos, A. Bachoumis, N. Andriopoulos, M. K. Birbas, and A. Birbas, "Deep Learning-based Application for Fault Location Identification and Type Classification in Active Distribution Grids," *Applied Energy* (Preprint), Mar. 2023.
- [3] J. Wang, H. Mokhlis, N. N. Mansor, H. A. Illias, A. K. Ramasamy, X. Wu, and S. Wang, "Smart Fault Detection, Classification, and Localization in Distribution Networks: AI-Driven Approaches and Emerging Technologies," *IEEE Access*, vol. 13, pp. 141664–141693, 2025, doi: 10.1109/ACCESS.2025.3596791.